

# RECENT DEVELOPMENTS IN SUPERCONDUCTING RF FREE ELECTRON LASERS

Lia Merminga<sup>†</sup>

Jefferson Laboratory, Newport News, VA 23606, USA

## Abstract

Superconducting RF (SRF) Free Electron Lasers (FELs) worldwide are reviewed. Two examples of high performance SRF FELs are discussed in detail: First, the Tesla Test Facility (TTF) FEL at DESY, which recently demonstrated Self Amplified Spontaneous Emission (SASE) saturation at the wavelength of 98 nm, an important milestone towards X-ray FELs in the Ångström regime. Second, the Jefferson Lab IR FEL, which recently lased with 2.1 kW of average power while energy recovering 5 mA of average current, an important milestone towards high average power FELs and towards Energy Recovering Linacs (ERLs) in general. We discuss the scientific potential and accelerator physics challenges of both classes of SRF-driven FELs.

## 1 INTRODUCTION

The superconducting rf linac has played an important role in the early development of FELs. Due to the special characteristics of SRF linacs, which include long pulse or CW operation, high efficiency, high gradient-low impedance structures, the development of new FEL facilities has continued and, within the past ~2 years, SRF-driven FELs have reached unprecedented values in FEL wavelength and FEL average output power. As progress in rf superconductivity continues to be dramatic, it is expected that SRF linacs not only will play an important role in future FEL development, but they may become the technology of choice for FEL driver accelerators.

After a brief introduction to FELs, this paper reviews the existing and planned SRF FEL facilities worldwide. It is fascinating to account that as recently as 1998, there were only two operating FEL facilities worldwide driven by SRF linacs, the pioneering FEL at Stanford and the Darmstadt S-DALINAC FEL. Today there are 6 existing (and more planned) SRF-driven FELs at Darmstadt, Rossendorf and DESY in Germany, JAERI in Japan and Jefferson Lab in the United States [1].

To illustrate the potential of SRF-driven FELs, the rest of the paper focuses on two examples of high performance SRF FELs. The first is the DESY TTF-FEL, which demonstrated SASE at the shortest wavelength to date at 98 nm. We discuss the range of possible scientific explorations that can only be realized with the expected characteristics of SASE devices. We review the accelerator physics challenges that SASE FELs present as they enter an unexplored domain of accelerator and FEL

physics. The second example of high performance SRF FEL is the Jefferson Lab (JLab) IR FEL, which has demonstrated energy recovery at the highest current to date of 5 mA. The success of the JLab IR FEL has inspired the conception of many new proposals and conceptual designs based on energy recovering linacs. These new designs push the envelope of energy recovery in various directions. We review these proposed designs, and then expand on the concept of energy recovery and outline the accelerator physics challenges of energy recovering linacs and the work that is going on at Jefferson Lab to address them. We conclude with an outlook towards the future.

## 2 FREE ELECTRON LASERS

Free Electron Lasers are sources of tunable, coherent radiation at wavelengths varying over a wide range from mm wave to the vacuum UV and soft X-rays. An FEL consists of an electron accelerator and a “wiggler” magnet. The magnetic field of the wiggler causes the electrons to oscillate transversely and radiate. These waves bunch the electrons causing them to radiate coherently near a resonant wavelength. In the oscillator configuration, the laser light reflects back and forth between the mirrors, gaining strength on each pass through the wiggler. At ultra short wavelengths, less than 100 nm, mirrors are not available. In this case, coherent bunching of the electron beam develops in a single-pass through the wiggler. In this “high gain mode” the radiation field amplitude grows exponentially with distance along the undulator. The exponential growth rate of the radiation field amplitude  $E$  is given by,

$$E \approx E_0 \exp[2\pi\rho\sqrt{3}N_w]$$

where  $N_w$  is the number of wiggler periods and  $\rho$  is the Pierce parameter given by [2]

$$\rho = \left( \frac{K}{4\gamma} \frac{\Omega_p}{\omega_0} \right)^{2/3}.$$

Here  $\omega_0 = 2\pi c/\lambda_w$ ,  $\lambda_w$  is the wiggler wavelength,  $\gamma$  is the relativistic energy of the electron beam, and  $K$  depends exclusively on parameters of the wiggler. Also  $\Omega_p = (4\pi e^2 n_e / \gamma)^{1/2}$  is the plasma frequency of an electron beam of particle density  $n_e$  and energy  $\gamma$ . In several cases, such as the DESY TTF-FEL, there is no “seed” light wave and thus radiation must grow from spontaneous emission. This process is referred to as Self-Amplified-Spontaneous-Emission and FELs based on the SASE principle are presently considered the most attractive

<sup>†</sup>merminga@jlab.org

candidates for extremely high brilliance coherent light with wavelength in the Ångström regime.

FELs impose stringent requirements on the electron beam properties. The energy is determined by the required wavelength via the resonance condition

$$\lambda_\gamma = \frac{\lambda_w(1+K^2)}{2\gamma^2} ,$$

where  $\lambda_\gamma$  is the resonant optical wavelength and the rest of the symbols have been defined earlier. For a given wiggler design, the average current  $I_{ave}$  is determined by the required FEL output power,

$$P_{FEL} = \eta_{FEL} I_{ave} E_{beam} ,$$

where  $\eta_{FEL}$  is the FEL extraction efficiency and  $E_{beam}$  is the electron beam energy. The bunch charge and bunch length are determined by the peak current required for sufficient gain. The emittance and energy spread are determined by the FEL interaction. For optimum coupling, the optical beam must overlap the electron beam through the wiggler. This requirement imposes a constraint on the geometric emittance of the electron beam,

$$\varepsilon \leq \frac{\lambda_\gamma}{4\pi} .$$

To ensure that all electrons radiate within the bandwidth of the FEL, the energy spread of the electron beam must also remain below a certain value,

$$\frac{\sigma_E}{E} < \frac{1}{5N_w} , \quad \frac{\sigma_E}{E} < \rho ,$$

for oscillators [3], and amplifiers [4] respectively. Finally for many applications short bunches at the sub-ps level are desirable.

Linacs in general and SRF linacs in particular can deliver beams, which satisfy these requirements [5]. In linacs the emittance and energy spread are determined by the injector, as opposed to storage rings where the equilibrium between synchrotron radiation excitation and damping sets a limit in the 6D phase space volume. In linacs sub-ps bunches are possible, whereas in storage rings typical rms bunch lengths are not shorter than about 10 ps. For long pulses or cw operation, SRF linacs have a clear advantage. High-gradient, low-impedance SRF structures allow the preservation of the exceptional beam quality required for very short wavelength FELs. Linacs can ensure exceptional amplitude and phase stability of the rf fields, at the  $10^{-5}$  level for CEBAF [6], thereby ensuring minimum contribution to the energy spread. Linacs in general demonstrate operational flexibility; changes in beam energy, bunch length, pulse patterns are all possible and easy to make. Finally energy recovered SRF linacs may be highly efficient accelerators.

## 3 EXISTING AND PROPOSED SRF FEL FACILITIES

### 3.1 Amplifiers

Table 1 shows the existing and planned SRF FEL facilities worldwide. We start with amplifiers. The only existing SRF SASE FEL is the DESY TTF-FEL [7,8] shown schematically in Fig. 1. It is driven by 1300 MHz TESLA cavities. The TTF-FEL has lased over a wavelength range from 80 nm to 180 nm, corresponding to a beam energy range between 181 and 272 MeV, and has demonstrated SASE saturation at the wavelength of 98 nm (See Fig. 2). Figure 3 shows the SASE spectrum at  $\lambda \sim 105.4$  nm. The peak current during lasing is 500A, and the rms bunch length is 1 ps. At a bunch charge of 1 nC, the measured normalized emittance from the gun is 3.5 mm mrad, and at the undulator entrance is 8 mm mrad. It should be noted that the TTF injector was not optimized for small emittance.

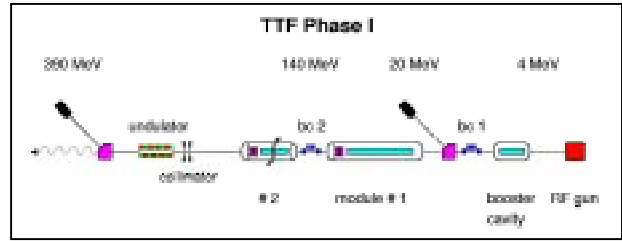


Figure 1: Schematic layout of the TESLA Test Facility Phase I (TTF1). (Courtesy of DESY TTF-FEL Group)

The TESLA Test Facility FEL will be upgraded to 1 GeV electron beam energy. The installation of an additional bunch compressor and an improved injector scheme are expected to allow 2500 A peak current and normalized emittance of 2 mm mrad. The expected minimum wavelength is 6 nm, with the use of a 30 m undulator. After the upgrade, the TTF FEL will be converted into a SASE FEL User Facility.

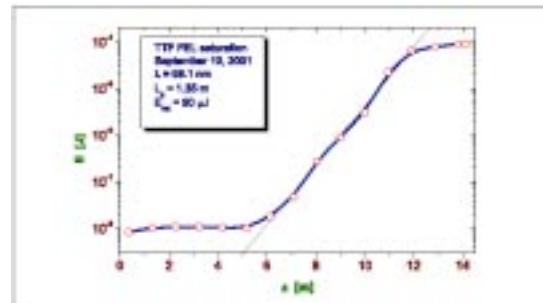


Figure 2: Energy of laser pulses (log scale) vs. position in the undulator.

DESY has proposed the construction of the XFEL [7], a SASE FEL to be integrated with the  $e^+e^-$  linear collider and designed to reach 1 Ångström radiation. A schematic layout of the TESLA XFEL is shown in Fig. 4. The

required beam energy is 35 GeV, the peak current is 5000 A and the rms bunch length is 80 fsec. The normalized emittance of the TESLA XFEL must be approximately 1 mm mrad at the gun and 1.6 mm mrad at the undulator entrance. Overall, the TESLA XFEL has to achieve a factor of 2 to 10 more stringent specifications in most key parameters compared to demonstrated performance at TTF or elsewhere. The major beam dynamics issues that must be resolved are outlined later.

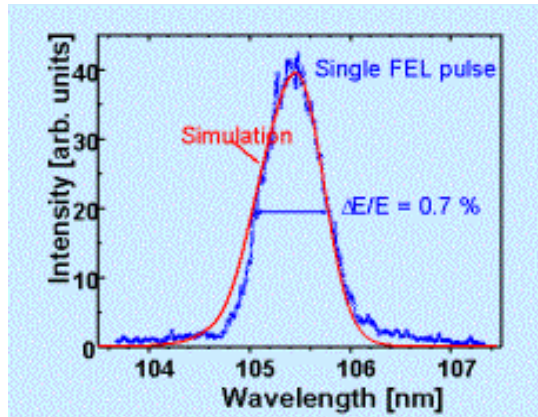


Figure 3: DESY TTF-FEL SASE spectrum at 105.4 nm. (Courtesy of DESY TTF-FEL Group)

The Berliner Electronenspeicherring-Gesellschaft für Synchrotronstrahlung (BESSY) proposes the construction of a linac-based, single-pass FEL user-facility for photon energies from 20 eV to 1 keV corresponding to wavelengths between 63 and 1.2 nm [9]. The expected pulse durations are less than 200 fs rms initially and ultimately possibly less than 20 fs. The 260 m long SRF linac will accelerate electrons up to 2.25 GeV. In the first phase of the project three undulators will be fed with electron beam extracted from the linac at 0.7-, 1.1-, and 2.25 GeV. To take full advantage of the superconducting linac it is planned to operate the rf in the accelerator in CW mode. This scheme allows for flexible time structures and more straightforward stabilization scheme of the electron beam energy. Plans aimed towards optimizing the scientific potential of this user-facility include

shortening of the photon pulse duration down to the 20 fs range, an improvement of the spectral purity, synchronization of the FEL with conventional laser sources and an increase of the overall output power. At present, a three year design-stage is funded as a collaboration between BESSY, DESY, the Hahn-Meitner-Institute Berlin, and the Max-Born Institute Berlin.

### 3.2 Oscillators

To date there are four laboratories with SRF-driven FEL oscillators that have produced light: Stanford, Darmstadt, JAERI and Jefferson Lab, and two laboratories with FELs in the construction or commissioning stage: Rossendorf (ELBE) and Jefferson Lab (IR FEL Upgrade and UV FEL). The Stanford SCA/FEL is driven by a superconducting linac, which operates at 1300 MHz and provides a 200  $\mu$ A electron beam of high quality at energies from 15 MeV to 45 MeV [10]. The electron beam is used to drive both a mid-infrared and a far-infrared FEL simultaneously, thereby covering wavelengths from 3-13  $\mu$ m and 15-65  $\mu$ m. The picosecond pulse train produced by the rf linac is well suited to ultra fast time domain studies. At the Stanford FEL Center comprehensive studies of vibrational dynamics in condensed matter systems have been performed for the first time. Other important experiments include infrared near-field spectroscopy of single living cells and synchronous pumping of an external optical cavity.

The S-DALINAC FEL at Darmstadt is driven by a CW recirculating linac operating at 3 GHz using 20-cell rf cavities. Due to the limited beam current it was a challenge to start the FEL, and it is likely that this device still has the lowest single pass gain of all linac-based FELs. The S-DALINAC FEL is used for experiments on the ablation of soft tissue. The possibility of increasing the FEL efficiency by dynamic tapering of the undulator is being explored [11].

The JAERI-FEL facility, shown schematically in Fig. 5, is driven by a superconducting linear accelerator with frequency of 499.8 MHz and has been developed to provide a quasi-cw far infrared (FIR) laser of a 1 ms long macropulse at 10 Hz repetition rate. Recently a high

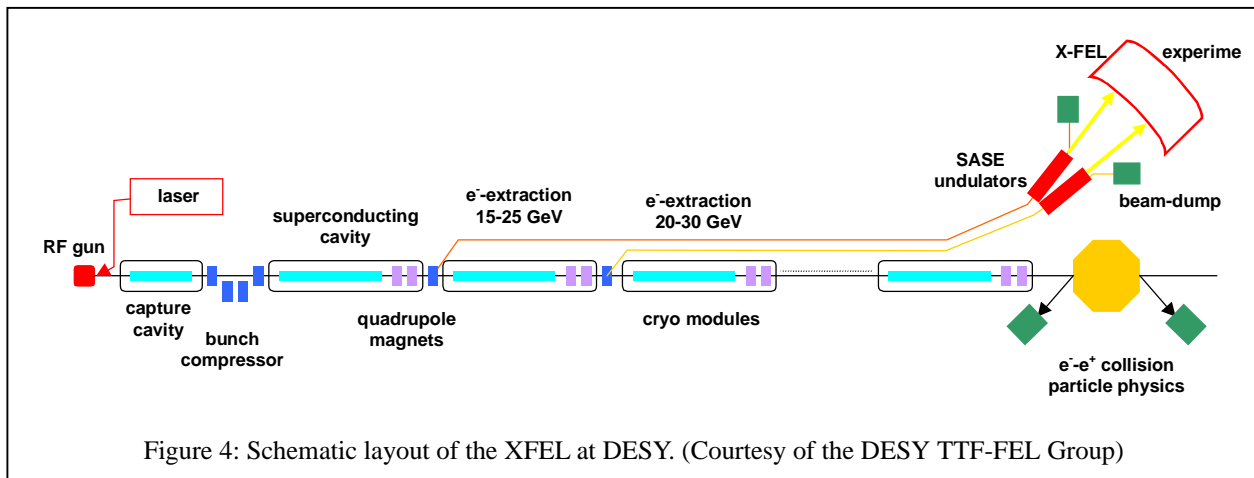


Figure 4: Schematic layout of the XFEL at DESY. (Courtesy of the DESY TTF-FEL Group)

Table 1: Existing (incl. under construction) and proposed (in italics) SRF FEL facilities worldwide

Amplifiers					
FEL	Accel/Freq [MHz]	Wavelength [ $\mu\text{m}$ ]	Energy [MeV]	Peak Current [A]	Bunch Length (rms) [psec]
TTF-FEL (DESY)	Linac/1300	0.08-0.18	181-272	500	1
<i>XFEL (DESY)</i>	<i>Linac/1300</i>	<i>0.0001</i>	<i>35000</i>	<i>5000</i>	<i>0.08</i>
<i>BESSY FEL</i>	<i>Linac/1300</i>	<i>0.045-0.0012</i>	<i>450-2200</i>	<i>5000</i>	<i>0.07</i>
Oscillators					
SCA FEL (Stanford)	Linac/1300	3-13/15-65	22-45/15-32	10/14	0.5-12/1-5
S-DALINAC (Darmstadt)	Recirculating Linac/3000	6-8	25-50	2.7	2
JAERI-FEL (Tokai)	Linac / 500 (ERL)	22	16.5	100	5
JLAB IR FEL	ERL/1500	1-6	48	60	0.4
JLAB IR FEL UPGRADE & UV FEL	ERL/1500	0.2-1	160	270	0.2
ELBE (Rossendorf)	Linac/1300	5-300	4-250	-	0.5-10

extraction efficiency, up to 6%, was demonstrated in the JAERI-FEL oscillator. A simultaneous measurement of FEL power and absolute detuning length of the optical cavity has shown that the FEL efficiency becomes maximum at the perfect synchronism and the lasing is sustained (Fig. 6). In the past it had been considered that only a transient state exists at zero detuning due to the laser lethargy effect [12]. This new mode of FEL lasing is possible due to the high brightness electron bunches, long macropulses and small timing jitter, demonstrating the capabilities of SRF accelerators. The plan is to commission the system with energy recovery this year [13].

The Jefferson Lab IR FEL, shown schematically in Fig. 7, is driven by a 1500 MHz superconducting rf energy recovering linac, has lased in the 1-6  $\mu\text{m}$  wavelength range and has reached average output power of 2.1 kW CW, the highest average power ever to be achieved [14].

The Jefferson Lab IR FEL Upgrade project is in the installation stage. The final energy of about 160 MeV will

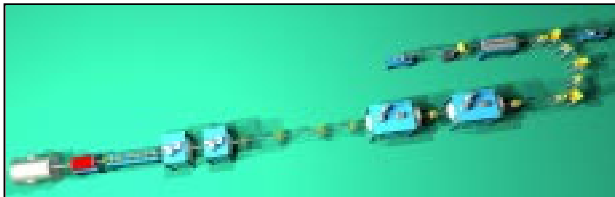


Figure 5: Schematic layout of the JAERI-FEL facility. (Courtesy of R. Hajima, JAERI)

be reached with the addition of two cryomodules, one old-style consisting of 5-cell cavities, and one new consisting of 7-cell cavities. The average current will be 10 mA, and the resulting average FEL power is expected to be >10 kW in the IR and >2 kW in the UV wavelengths [15,16].

The ELBE FEL facility at Rossendorf has a CW 1300 MHz linac and two undulators that will allow access to a wide range of wavelengths. The linac is presently being commissioned [17].

In the following we focus on two examples of high performance SRF FELs: The DESY TTF-FEL and the JLAB IR FEL. Both FELs have shown unprecedented

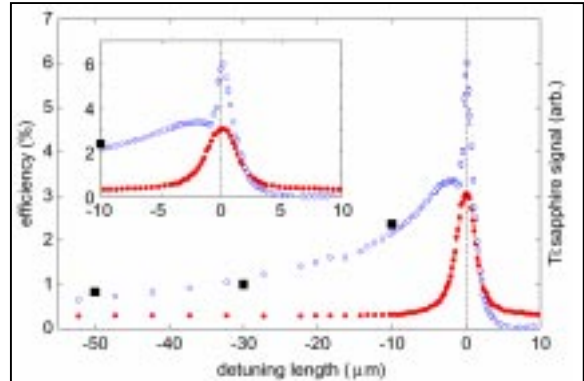


Figure 6: JAERI-FEL efficiency (open circle) and Ti:sapphire signal (solid circles) vs. detuning length. The enlargement around  $\delta L=0 \mu\text{m}$  is shown. (Courtesy of R. Hajima, JAERI)

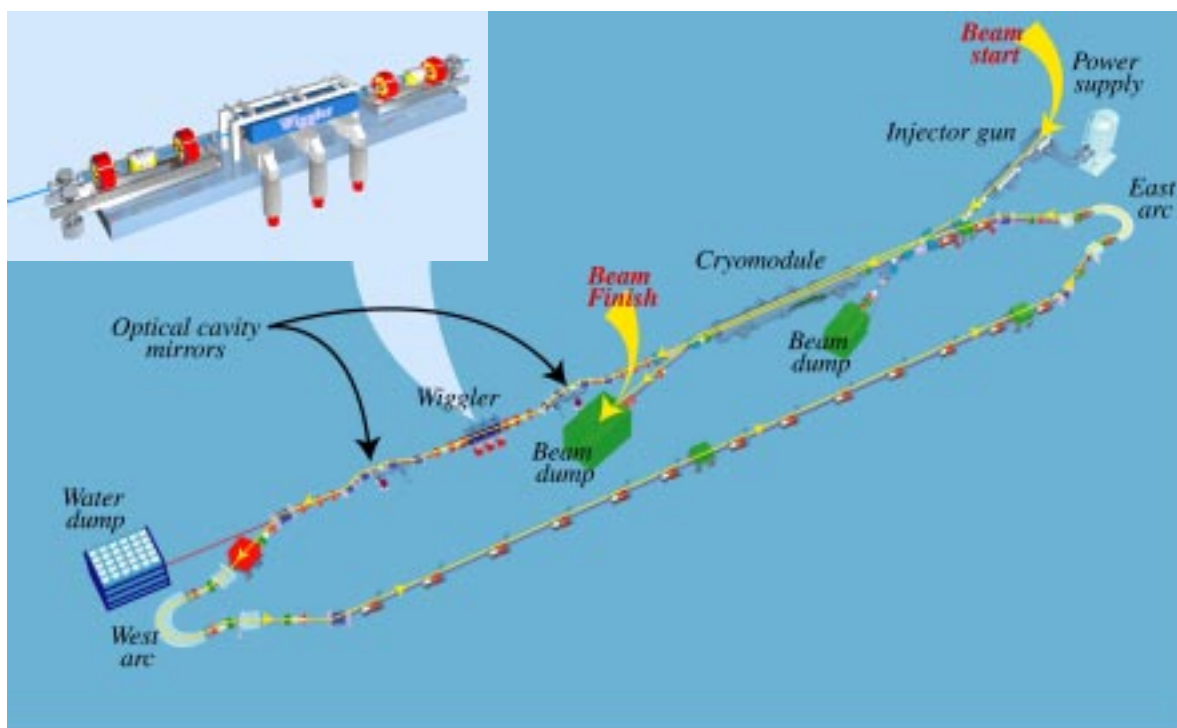


Figure 7: The Jefferson Lab IR FEL.

performances, both hold great promise for the future and both present accelerator and FEL physics challenges.

## 4 THE DESY TTF-FEL AND SASE FELS

### 4.1 Scientific Reach of SASE FELs

The DESY TTF-FEL with its pioneering performance holds the promise that SASE-FELs at wavelengths in the Ångström regime, where the XFEL is designed to operate, are feasible. Moreover the scientific case of the XFEL includes a wide range of applications not possible today [8].

X-ray lasers have been contemplated for years as probing tools because they would combine the outstanding properties of laser light with the atomic resolution (the X-ray wavelength, which determines the smallest distance one can study with such a probe, is comparable to the atomic dimension) and the penetration power offered by X-rays.

The brilliance, coherence and timing –down to the femtosecond regime– are all properties that will allow a wide range of novel ideas to be explored with an X-ray FEL. The range of applications includes: the investigation of structural changes on ultra short time scales, the nonlinear interaction of X-rays and matter – leading to multiphoton processes in atoms and molecules, which can not be studied with the present radiation sources – and, by focusing the X-rays down to  $\mu\text{m}^2$  or less, one will generate plasmas at still totally unexplored temperatures and pressures.

Perhaps one of the most fascinating applications of X-ray FELs comes from life sciences. At the present time an

exponentially increasing number of biological structures are solved and deposited at the protein data bank and in all likelihood this trend will continue. However, it is anticipated that many of today's challenges in structural biology will persist. These include systems that are difficult to crystallize, such as membrane proteins and large multicomponent complexes, of which only a few have been solved by now. Membrane proteins naturally have almost no tendency to form three-dimensional crystals, which are required for their crystallographic structure determination.

Furthermore, the study of the structure of large macromolecular assemblies, such as the ribosome, a very large but relatively stable protein-RNA assembly, is one of the keys to gaining insight into the interplay of different proteins and will facilitate the understanding of biological processes on a molecular or even atomic level. It will help to address the fundamental question of how biology works on a molecular scale. The problem is that the crystallization of such large assemblies is difficult. In addition, for a detailed understanding of the function of proteins, the knowledge of the dynamical behavior is as important as the three-dimensional static structure. An X-ray FEL with the powerful radiation of  $1 \text{ \AA}$  wavelength and very short pulse length of  $\leq 100 \text{ fs}$ , could overcome these limitations and allow the exploration of both the structure and the dynamics of complex biological systems with unprecedented detail.



## 4.2 Accelerator Physics Challenges of SASE FELs

The SASE FEL process requires high peak currents (several kA) and very small normalized transverse beam emittance, of order 1 mm mrad. As an electron gun that delivers ultra short bunches with very small emittance does not exist, the SASE FEL requirements are met by generating bunches of small emittance from an rf photocathode which are subsequently compressed longitudinally at high energy using a magnetic chicane. A strong rf field at the cathode provides rapid acceleration to relativistic energies to reduce space-charge effects, which can blow up the beam. During off crest acceleration, a correlated energy distribution is generated within the bunch, which results in bunch compression after the beam is propagated through a magnetic bypass to bring head and tail of the bunch closer together. Clearly the goal is to preserve the low beam emittance from the gun to the undulator entrance. Apart from the space-charge forces, wakefields and coherent synchrotron radiation (CSR) can seriously degrade the beam emittance.

An intense bunch of particles traveling through an accelerating structure excites wakefields, which act back on the bunch itself. When a bunch travels off-axis in a cavity, the transverse wakefields will deflect the tail of the bunch away from the axis, resulting in an increase of the total transverse phase space area occupied. Although still important, this effect is smaller in superconducting rf cavities than in normal conducting rf cavities. Because of the exceedingly low surface resistance of superconducting cavities, the dissipated power is not an overriding issue, therefore superconducting cavities can have large apertures, which result in reduced coupling impedance of higher order modes; for transverse modes this coupling can be an order of magnitude below that expected for an optimized room temperature cavity.

The greatest concern regarding emittance preservation in SASE FELs is bunch compression. When a bunch goes through a bend, each electron radiates. When the radiation wavelength is longer than the bunch length, the radiation from individual electrons adds constructively to form coherent synchrotron radiation. These CSR fields acting on the short bunches in the chicanes can increase the transverse emittance by orders of magnitude; therefore a careful design optimization is required.

Additional challenges of SASE FELs include the requirement on the electron beam orbit to be straight within the undulator in order to guarantee permanent overlap with the radiation field. The associated tolerance for the XFEL is about 10  $\mu\text{m}$  over 100 m! The rf stability and timing, required for small energy width (of order  $10^{-4}$ ) to ensure that all electrons radiate within the bandwidth of the FEL must be exceptionally good. Finally electron beam diagnostics for the ultra short, high-brightness bunches need to be developed. In short, SASE FELs enter a new domain of accelerator physics and the issues are being addressed vigorously in laboratories and institutions worldwide.

## 5 THE JEFFERSON LAB IR FEL AND ENERGY RECOVERING LINACS

### 5.1 Scientific Reach of High Power IR FELs

The JLab IR FEL is a groundbreaking accelerator and FEL. Its performance holds the promise that high power FELs and ERLs in general are feasible at much higher current and power levels. Moreover, the JLab IR FEL has enabled a rich applied and basic science program, which includes the investigation of both linear and nonlinear phenomena in materials as diverse as proteins and metals, pulsed laser ablation and deposition, laser nitriding, synthesizing carbon nanotubes and micromachining [18]. Linear dynamics using pump-probe techniques has been applied to amide-I absorption at 5 to 8 mm in proteins, and to hydrogen defects in silicon at 3 mm [19, 20]. Research is planned to investigate nonlinear interactions in metals and gases, and to study phenomena that determine ablation rates – such as multiphoton absorption. Subpicosecond time structure is critical in defining these fast, dynamic processes. In the following we expand on some of these applications of a high power, high repetition rate IR FEL.

Pulsed laser ablation and deposition is a potential applied-science application for manufacturing large-area films. The FEL's ultra fast pulses offer a low ablation threshold, substantially lessened target damage, and particulate elimination. High repetition rate implies high deposition rate, and may mean greater control over ablation and growth dynamics. Wavelength tunability results in enhanced ablation and deposition with resonant absorption, such as in polymers, using specific resonances to control growth processes.

Laser nitriding is a method of modifying the properties of metals to obtain a harder surface with better corrosion resistance and the ability to hold higher standoff voltages. The JLab FEL was successfully used to produce high-quality nitride films on iron, titanium, and silicon.

Carbon nanotube structures present a range of production challenges that might be circumvented or better understood by use of the JLab FEL's repetition rate, wavelength tuning and power. Studies are underway to determine how the structures are formed and discover optimum conditions for making them with tailored properties, as well as to learn more about real-time process monitoring and control. The JLab FEL with 3  $\mu\text{m}$  light at 400 to 600 W average power has synthesized single-wall carbon nanotubes, with smaller diameters than nanotubes produced by direct current arc or table-top pulsed laser vaporization, and production rates measured in mg/rams per minute rather than mg/rams per hour [21].

Micromachining is an industrial application applied on metals for automotive engine applications, and also on glasses and ceramics for the fabrication of true three-dimensional microstructures. With nano-scale engineering of key features, it is hoped that satellites could be reduced to the size of baseballs or smaller.

## 5.2 Recent Trends in Energy Recovering Linacs

From accelerator physics point of view the success of the JLab IR FEL has inspired a number of proposals and conceptual designs that are based on energy recovering linacs [22]. Cornell University in collaboration with Jefferson Lab, has proposed the ERL [23], a synchrotron radiation light source driven by an energy recovering SRF linac operating at an energy of 5-7 GeV and an average current of 100 mA. A proposal for a smaller scale prototype, 100 MeV and 100 mA, to address accelerator physics issues has been submitted to NSF [24]. Brookhaven National Laboratory is proposing a similar type of light source, the PERL Light Source, driven by a 1300 MHz, 3 GeV SRF linac. The average current is 200 mA with 150 pC per bunch at 1.3 GHz repetition rate [25]. Lawrence Berkeley National Lab is proposing the construction of a facility to produce femtosecond x-ray pulses with high flux, and repetition rate matched to the requirements of structural dynamics experiments. The facility uses a 1300 MHz SRF recirculating linac for acceleration (and deceleration) of electrons produced by a high-brightness photocathode rf gun, at a bunch repetition rate of approximately 10 kHz [26]. An energy recovering SRF linac has been proposed as an electron cooling device for the cooling of the ion beam at RHIC to achieve higher luminosity [27]. Finally, energy recovering linac-on-ring scenarios for electron-ion colliders are examined as alternatives to ring-ring scenarios [28, 29]. All these designs push the envelope of energy recovery in various fronts. An important question therefore is: “Where is the limit of energy recovery?” The next section attempts to shed light on this question.

## 5.3 Accelerator Physics Challenges of ERLs

Energy recovery has worked extremely reliably in the Jefferson Lab FEL with beam current up to 5 mA, for both pulsed and CW beams. Figure 8 shows the klystron drive signals for the gradient feedback loop, for four of

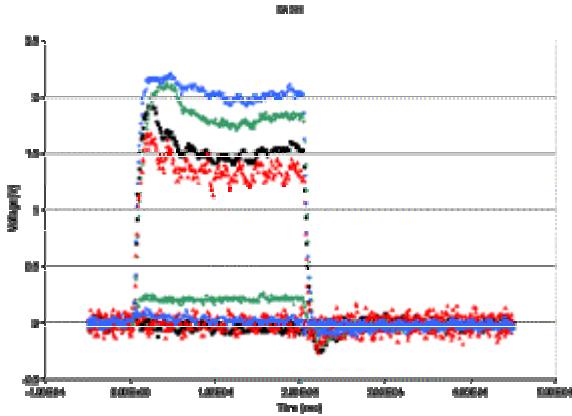


Figure 8: Energy recovery with pulsed beam: Response of the gradient loop drive signals, in four rf cavities, to a 200  $\mu$ sec beam pulse, with ( $\sim 0$  Volts) and without ( $\sim 2$  Volts) energy recovery.

the IR FEL linac rf cavities. When a 200  $\mu$ sec beam pulse is injected in these cavities, in the absence of energy recovery, the gradient drive signals reach  $\sim 2$  V to compensate for beam loading. With energy recovery, these signals are close to 0 V (where 0 V corresponds to the DC voltage required to drive the accelerating field in the cavity), as the decelerating and accelerating beam vectors cancel each other resulting in nearly zero net beam loading. Figure 9 is a plot of the rf power required to accelerate up to 3.5 mA of CW beam current compared to the power required for no beam, in each of the 8 cavities. The required rf power is nearly independent of beam current, which, in addition to the direct savings having to do with rf power and rf capital equipment, also increases the overall system efficiency. Furthermore, the reduced electron beam power (by the ratio of the highest to the injected beam energy) that must be disposed of at the beam dumps makes the dump design easier and less costly.

To quantify the efficiency of energy recovering linacs we have introduced the concept of “rf to beam multiplication factor”  $\kappa$ , defined as  $\kappa \equiv P_{beam}/P_{RF}$ , the ratio of the beam power at its highest energy  $E_f$  to the rf power required to accelerate the beam to  $E_f$ . For an electron beam of average current  $I_b$ , injected into the ERL at injection energy  $E_{inj}$ , and in the limit of perfect energy recovery (exact cancellation of the accelerating and decelerating beam vectors), the multiplication factor is equal to

$$\kappa \equiv \frac{P_{beam}}{P_{RF}} \approx \frac{JE_f}{(J-1)E_{inj} + E_f}$$

where the normalized current  $J$  is given by,

$$J = \frac{4I_b(r/Q)Q_L}{G_a}$$

$Q_L$  is the loaded quality factor,  $G_a$  is the accelerating gradient and  $(r/Q)$  the shunt impedance per unit length of the linac rf cavities. For parameters close to the Cornell ERL [23] design:  $Q_L = 2 \times 10^7$ ,  $G_a = 20$  MV/m,  $(r/Q) = 1000$   $\Omega/m$ ,  $E_{inj} = 10$  MeV and  $E_f = 7$  GeV, the multiplication factor  $\kappa$  is  $\sim 500$  for beam currents of  $\sim 200$  mA, approaching efficiencies typical of storage rings, while maintaining beam quality characteristics of linacs, namely emittance and energy spread determined by the source and the ability to have sub-picosecond short bunches.

The multiplication factor  $\kappa$  increases as function of the

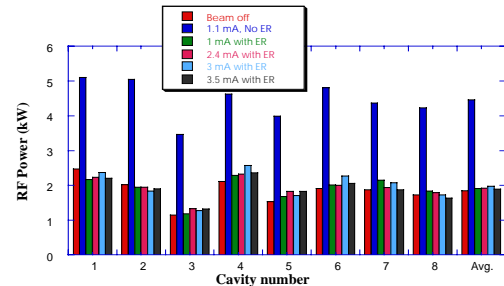


Figure 9: RF power requirements in the linac cavities for a range of beam currents.

loaded quality factor  $Q_L$  of the superconducting cavities in the ERL. The higher the  $Q_L$ , the higher the overall ERL efficiency. An important question that arises is how high can  $Q_L$  be. A high  $Q_L$  implies a narrow resonance of the superconducting cavity, therefore microphonic vibrations can cause large phase and amplitude fluctuations that need to be corrected if a certain value of the energy spread is to be maintained at the exit of the linac. Furthermore, for high gradient, high  $Q_L$  cavities, the radiation pressure during gradient turn-on can shift the resonant frequency of the cavity by several bandwidths of the cavity, resulting in operational difficulty and, under certain conditions, unstable behavior [30]. To date, no experience exists with regulation of high gradient cavities with  $Q_L \geq 10^7$ . Several rf control system concepts have been proposed, including the self-excited loop, the generator driven system and a hybrid of the two [31]. Ideas for active suppression of microphonic noise and Lorentz force detuning using piezo elements are also being explored [32].

The multiplication factor also increases with the average beam current, and asymptotically approaches a value that is equal to the ratio of highest to injected beam energy,  $E_f/E_{inj}$ . The higher the beam current is, the higher the overall system efficiency becomes. At increased beam current a number of collective effects, driven predominantly by the high- $Q$  superconducting rf cavities, become important and can potentially limit the average current. In a recirculating linac, there is a feedback system formed between the beam and the rf cavities, which is closed and instabilities can arise at sufficiently high currents. Instabilities can result from: a) the interaction of the beam with transverse Higher Order Modes (HOMs) (transverse Beam Breakup (BBU)) [33,34], b) the interaction of the beam with longitudinal HOMs (longitudinal BBU) [35], and c) the interaction of the beam with the fundamental accelerating mode (beam-loading instabilities) [36]. The basic mechanism of all three types of multibunch instabilities is fundamentally the same.

In the case of transverse BBU, a beam entering an rf cavity on axis can be deflected either horizontally or vertically by a previously excited HOM. When the beam returns to the same cavity displaced, due to the optics of the recirculator (non-zero  $M_{12}$  or  $M_{34}$  transfer matrix elements), it can exchange energy with the HOM in a way that excites the HOM and can now further deflect subsequent bunches until they hit the beam pipe.

The mechanism of the longitudinal BBU is analogous to that which generates the transverse BBU, where now the important element of the optics design is the isochronicity ( $M_{56}$  matrix element) of the recirculator. An important difference, however, is that the induced current can only achieve a value equal to the average beam current, whereby saturation will occur [35].

Beam-loading instabilities can arise from fluctuations of the cavity fields. Energy changes can cause beam loss on apertures, phase oscillations and optical cavity detuning. These effects can in turn cause changes in the laser output

power through the FEL gain function. All three effects – beam loss, phase shifts and laser power variations – change the beam-induced voltage in the cavities through the recirculating beam, hence the term “beam-loading instabilities.” If the rf feedback does not have sufficient gain and bandwidth, the change in the beam-induced voltage will further change the cavity voltage in a way that amplifies the energy error of the electron beam and drives the loop unstable. For CW accelerators the beam-loss instability is of no practical interest because losses can never be high enough to induce the instability before operation ceases.

Of the three types of multibunch instabilities, transverse BBU appears to be the limiting instability in recirculating, energy recovering linacs [37]. The longitudinal BBU appears to have the highest threshold current because typical values of  $M_{56}$  are an order of magnitude smaller than  $M_{12}$  or  $M_{34}$ , while typical damping of the strongest longitudinal HOMs is at the  $10^4$ -  $10^5$  level, similar to the transverse HOMs. The beam loading instabilities can exhibit open loop threshold currents close to the design currents contemplated in upcoming ERL projects. However, the low level rf control feedback raises the threshold by more than an order of magnitude [36].

The theory and simulations of these instabilities are quite mature. However, no experimental verification of the theoretical models exists despite previous attempts [38] that took place in the Injector of the CEBAF accelerator. The Jefferson Lab IR FEL provided a unique test bed to experimentally verify a number of these effects.

The experiments that were carried out in the Jefferson Lab IR FEL included an attempt to induce the BBU instability, and measurements of the beam transfer functions in the recirculation mode. The first experiment consisted of both changing the optics of the recirculator so that larger beta functions at the cavity locations were obtained, and lowering the injection energy into the linac to 5 MeV and the final energy to 20 MeV. Under these conditions the predicted threshold was just under 5 mA. However during the execution of the experiment, the magnified beta functions caused unacceptable beam loss that prohibited beam operations at current above 3.5 mA, and the instability was not observed.

The second experiment consisted of beam transfer function measurements in the recirculating mode. Although these measurements were performed at beam currents below the threshold current of the transverse BBU instability, yet they led to clear estimates of the instability threshold. Data were recorded by exciting different HOMs at several cavities, with different associated  $r/Q$  and  $Q$  values at two energies and several optics settings. The threshold current for each configuration was derived from nonlinear least-square fits to the data [39]. For the nominal FEL configuration the threshold was determined to be between 16 mA and 21 mA. This is to be compared with the theoretical prediction of 27 mA, obtained from the simulation code TDBBU



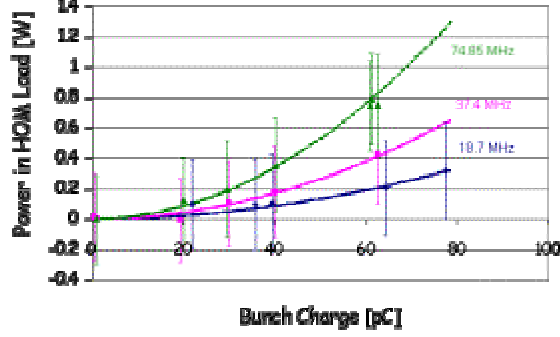


Figure 10: HOM power measured in one of the two HOM loads of the CEBAF 5-cell cavities vs. bunch charge for 3 different bunch repetition rates.

[34] and the matrix analysis code MATBBU [40], resulting in agreement at better than 40% level.

Another potential limitation of ERLs can originate in the excitation of HOMs by the high-current, short-bunch length beams in superconducting cavities. In addition to beam stability consequences, these HOMs could result in increased cryogenic load due to power dissipation in the cavity walls. At high currents, the amount of dissipated power can be significant. For example, for average current equal to 100 mA, bunch charge of 0.5 nC and  $k_{\parallel} = 10$  V/pC, the HOM power dissipation is approximately equal to 1 kW per cavity, in the energy recovery mode. In contrast, the maximum HOM power dissipated to date in the JLab IR FEL is approximately 6 W per cavity. The fraction of the power dissipated on the cavity walls depends on the bunch length and can potentially limit the peak and average current due to finite cryogenic capacity. According to BCS theory, the surface resistance of Nb increases  $\propto f^2$ , therefore the power dissipated in the cavity walls increases as the frequency of the electromagnetic radiation increases. According to an analytical model that assumes  $k_{\parallel} \propto 1/\sqrt{\sigma_z}$ ,  $\sim 70\%$  of the total HOM power is in frequencies above 10 GHz for  $\sigma_z = 1$  psec [41]. In the TESLA project, in addition to HOM filters used to extract the HOM power in frequencies up to  $\sim 20$  GHz to loads at room temperature, special absorbers are foreseen operating at 70 K and placed between cryomodules [42]. These cooled absorbers are expected to extract power in the range from a few GHz up to hundreds of GHz. The HOM power anticipated in the Cornell ERL is already  $\sim 100$  times higher than that of TESLA in the collider mode and cooled absorbers are foreseen between cavities. Finally the effect of losses in the frequency range beyond the threshold for Cooper pair breakup (about 750 GHz) in superconducting niobium has been investigated [43]. It was concluded that in a string of 9-cell cavities the temperature rise of the inner cavity surface and the resulting  $Q_0$  drop are negligible.

Experimental measurements of the HOM power dissipation under varying beam parameters were obtained at the JLab IR FEL. The amount of HOM power

transferred to the loads was measured and compared with calculations. Temperature diodes were placed on the two HOM loads of a linac cavity and temperature data were recorded for a range of values of charge per bunch at three values of the bunch repetition frequency, 18.7 MHz, 37.4 MHz and 74.85 MHz. Figure 10 displays the measured HOM power vs. charge in one of the two HOM loads per cavity, as well as least-square fits to the data constrained to a single value of the loss factor. The data are consistent with the calculated fraction of the HOM power absorbed by the loads, approximately 30% of the total power. At the present time no statement can be made about the amount of power dissipated in the cryogenic environment because no instrumentation was in place to measure it. Further experiments are planned to be executed in the Jefferson Lab 10 kW FEL Upgrade, designed to energy recover 10 mA average current and in the Cornell ERL Prototype, designed to energy recover 100 mA of average current.

## 6 CONCLUSIONS AND OUTLOOK

RF superconductivity is a key technology that enables and allows high performance driver accelerators for Free Electron Lasers and light sources. Two SRF-driven FELs have reached unprecedented performance in shortest wavelength and highest average laser power. Energy recovery is emerging as a potentially powerful application of rf superconductivity, largely due to the success of the Jefferson Lab IR FEL. High gradients with high associated cavity quality factors ( $Q_0$ ), better damping of HOMs and rf control in the presence of the highest possible loaded  $Q$  ( $Q_L$ ) of the cavities will allow the preservation of high brightness beams and open new possibilities in accelerator design and applications.

## 5 ACKNOWLEDGEMENTS

The author is grateful to the following individuals for providing information that was used in this paper: J. Rossbach and M. Koerfer (DESY); R. Swent and T. Smith (Stanford); D. Graef (Darmstadt); R. Hajima and E. Minehara (JAERI); P. Michel (Rossendorf); J. Knobloch and I. Bazarov (Cornell Univ.); J. Hajdu (Uppsala Univ.); and S. Benson, G. Krafft and G. Neil (Jefferson Lab). In addition, Steve Benson, Yu Chao, Jean Delayen and G. Krafft carefully read and commented on the manuscript. This work was supported by the USA DoE contract No. DE-AC05-84ER40150, the Office of Naval Research, Commonwealth of VA and the Laser Processing Consortium.

## 6 REFERENCES

- [1] W. B. Colson, "Short Wavelength Free Electron Lasers in 2000," Proc. of FEL Conference 2001.
- [2] R. Bonifacio, C. Pellegrini and L.M. Narducci, Opt. Commun. 50 (1984) 373.

- [3] G. Dattoli et al., "Intensity Saturation Mechanism in Free Electron Lasers," IEEE J. Quantum Elect. QE-28 (1992).
- [4] C. Pellegrini, "Progress Toward a Soft X-Ray FEL," NIM A272 (1988) 364-367.
- [5] H. A. Schwettman, "Superconducting Linacs as Free Electron Laser Drivers," IEEE Transactions on Applied Superconductivity, Vol. 9, No. 2, June 1999.
- [6] G. A. Krafft et al. "Measuring and Controlling Energy Spread at CEBAF," Proc. LINAC Conf. 2000.
- [7] J. Rossbach, "New Developments on Free Electron Lasers Based on Self-Amplified Spontaneous Emission," Proc. PAC'01, Chicago, June 2001.
- [8] TESLA Technical Design Report, Part V: The X-Ray Free Electron Laser, Eds: G. Materlik, Th. Tschentscher.
- [9] "Visions of Science: The BESSY SASE-FEL in Berlin-Adlershof," <http://www.bessy.de/FEL/sc/sc.html>
- [10] R. Swent, "Status of the Stanford Picosecond FEL Center," Proc. of FEL Conference 2000.
- [11] M. Brunken et al., "Status of the FEL at the S-DALINAC," Proc. of FEL Conference 2000.
- [12] N. Nishimori, R. Hajima, R. Nagai and E. J. Minehara, "Sustained Saturation in a Free-Electron Laser Oscillator at Perfect Synchronism of an Optical Cavity," Phys. Rev. Letters, Vol. 86, No. 25, pg. 5707, June 2001.
- [13] R. Hajima et al., "The JAERI energy-recovery linac: construction and testing status," Proc. of FEL Conf. 2001.
- [14] G. R. Neil, C. L. Bohn, S. V. Benson, G. Biallas, D. Douglas, H. F. Dylla, R. Evans, J. Fugitt, A. Grippo, J. Gubeli, R. Hill, K. Jordan, G. A. Krafft, R. Li, L. Merminga, P. Piot, J. Preble, M. Shinn, T. Siggins, R. Walker, and B. Yunn, "Sustained Kilowatt Lasing in a Free Electron Laser with Same-Cell Energy Recovery," Physical Review Letters Vol. 84, Number 4 (2000).
- [15] D. R. Douglas, S. V. Benson, G. A. Krafft, R. Li, L. Merminga, B. C. Yunn, "Driver Accelerator Design for the 10 KW Upgrade of the Jefferson Lab IR FEL," Proc. LINAC Conf. (2000).
- [16] S. V. Benson et al., "A 10 kW IRFEL Design for Jefferson Lab," Proc. of PAC Conf. 2001.
- [17] P. Michel et al., "First operation of the ELBE superconducting electron linear accelerator," Proc. FEL 2001.
- [18] H. F. Dylla, in Laser Focus World, August 2001.
- [19] R. Austin, Phys. Rev. Lett., 84, 5435 (2000).
- [20] M. Budde et al., Phys. Rev. Lett., 85, 1452 (2000).
- [21] A. Loper, et al., "Production of Single Walled Carbon Nanotubes using tunable radiation from a Free Electron Laser", March 2001 APS meeting, C20.002.
- [22] G. Neil, "Trends and Opportunities in Light Source Development," Proceedings of FEL Conference 2001.
- [23] I. Bazarov, S. Belomestnykh, D. Bilderback, K. Finkelstein, E. Fontes, S. Gray, S. M. Gruner, G. A. Krafft, L. Merminga, H. Padamsee, R. Helmke, Q. Shen, J. Rogers, C. Sinclair, R. Talman, and M. Tigner, "Study for a Proposed Phase I Energy Recovery Linac (ERL) Synchrotron Light Source at Cornell University", CHSS Technical Memo 01-003 and JLAB-ACT-01-04 (2001).
- [24] J. Knobloch "Future Light Source" these proceedings
- [25] I. Ben-Zvi, "Photoinjected Energy Recovery Linac R&D at Brookhaven National Laboratory," PERL Photoinjector Workshop, BNL (2001).
- [26] J. N. Corlett et al., "Initial Feasibility Study of a Dedicated Synchrotron Radiation Light Source for Ultrafast X-Ray Science", LBNL-48171, October 2001.
- [27] I. Ben-Zvi et al., "Electron Cooling For RHIC", Proceedings of PAC Conference (2001).
- [28] L. Merminga, G. A. Krafft and V. Lebedev, "An Energy Recovery Electron Linac-on-Proton Ring Collider," Proc. of 18<sup>th</sup> HEACC Conf., Japan (2001).
- [29] I. Ben-Zvi, J. Kewisch, S. Peggs, J. Murphy, "Accelerator Physics Issues in eRHIC," NIM A463, 94 (2001).
- [30] J. R. Delayen, "Phase and Amplitude Stabilization of Superconducting Resonators," California Institute of Technology Ph.D. Thesis (1978).
- [31] Low Level RF Workshop, Jefferson Lab, April 2001
- [32] M. Liepe, W.D. Moeller, S.N. Simrock, "Dynamic Lorentz Force Compensation with a Fast Piezoelectric Tuner," Proceedings of PAC Conference 2001.
- [33] J. J. Bisognano and R. L. Gluckstern, "Multipass Beam Breakup in Recirculating Linacs," Proc. PAC 1987.
- [34] G. A. Krafft and J. J. Bisognano, "Two-Dimensional Simulations of Multipass Beam Breakup," Proc. PAC 1987.
- [35] J. J. Bisognano and M. L. Fripp, "Requirements for Longitudinal HOM Damping in Superconducting Recirculating Linacs," Proc. LINAC Conf. 1988.
- [36] L. Merminga, P. Alexeev, S. Benson, A. Bolshakov, L. Doolittle and G. Neil, "Analysis of the FEL-RF Interaction in Recirculating, Energy-Recovering Linacs with an FEL," Nuclear Instruments and Methods A 429 58-64 (1999).
- [37] L. Merminga, "RF Stability in Energy Recovering Free Electron Lasers: Theory and Experiment," Proc. of FEL Conference 2001 to be published in NIM-A (2001).
- [38] N. Sereno, "Experimental Studies of Multipass Beam Breakup and Energy Recovery Using the CEBAF Injector Linac," Ph.D. Thesis, University of Illinois (1994) and N. Sereno et al., Proceedings of PAC Conference (1993).
- [39] L. Merminga, I. Campisi, D. Douglas, G. Krafft, J. Preble and B. Yunn, "High Average Current Effects in Energy Recovering Linacs," Proceedings of PAC Conference (2001).
- [40] B. Yunn and L. Merminga, Work in progress (2001).
- [41] L. Merminga, G. A. Krafft, C. W. Leemann, R. M. Sundelin, B. C. Yunn and J. J. Bisognano, "Specifying HOM-Power Extraction Efficiency in a High Average Current, Short Bunch Length SRF Environment," Proc. LINAC Conference (2000).
- [42] A. Joestingmeier, M. Dohlus, M. Wendt and C. Cramer, "Theoretical and Practical Investigations Concerning the Design of a HOM Broadband Absorber for TESLA," DESY TESLA-00-11 (2000).
- [43] R. Brinkmann et al., "THz Wakefields and their Effect on the Superconducting Cavities in TESLA," Proceedings of 7<sup>th</sup> EPAC Conference, Vienna (2000).